Rare Metal Materials and Engineering
Volume 52, Issue 3, March 2023
Available online at www.rmme.ac.cn

Science Press

Cite this article as: Cao Chao, Wang Jinxiang, Yang Ming, et al. Experiment and Numerical Simulation of Indium/Iron Composite Plate Prepared by Explosive Welding[J]. Rare Metal Materials and Engineering, 2023, 52(03): 883-889.

ARTICLE

Experiment and Numerical Simulation of Indium/Iron Composite Plate Prepared by Explosive Welding

Cao Chao[1], Wang Jinxiang[1], Yang Ming[1], Tang Kui[1], Fang Yu[2]

[1] National Key Laboratory of Transient Physics, Nanjing University of Science and Technology, Nanjing 210094, China; [2] Anhui Honlly Clad Metal Materials Technology Co., Ltd, Xuancheng 242000, China

Abstract: A novel explosive welding method was proposed to prepare the indium/iron composite plate by inserting a velocity-control plate between the explosive and composite plate to achieve the ideal welding condition. The experiments were conducted to investigate the effects of explosive load, and the parameters of explosive welding were calculated by the theoretic method. Numerical simulation of the smoothed particle hydrodynamics (SPH) method was used to verify the parameters and to investigate the formation mechanism of the bonding interface. The distributions of pressure and plastic strain were also studied. Results show that the wave structures become more obvious when the explosive thickness increases. The shear test results indicate that the shear strength of indium/iron composite plate is 16 MPa, which is higher than that of the indium material. After the three-point bending test, no cracks can be observed at the bonding interface. The modified explosive welding method can effectively prepare the high quality indium/iron composite plate.

Key words: explosive welding; indium/iron composite plate; velocity-control plate; SPH simulation

Indium (In), as a soft metal, is stable in the air and water at standard temperature and pressure, which has low resistivity, low melting point, and high ductility. Due to its good thermal and physical properties, indium has been widely used in the manufacture of solar cells, energy-efficient windows, and spectro-electrochemistry and organic light-emitting diodes. In aircraft industries, indium is commonly used in specific parts because it can prevent reactions with air and has fine wear resistance. In addition, the softness and low temperature workability of indium are favorable characteristics for service in vacuum systems, cryogenic pumps, and other unique situations[1–3]. However, the complex production process and high cost of indium restrict its applications. Due to its poor mechanical properties, indium is usually used in the form of indium-tin oxide and electroplating indium[4]. Iron (Fe) is widely used due to its good physical and mechanical properties. The indium/iron composite plate combines the good properties of both materials and can serve in different fields with relatively low cost, presenting a broad application prospect.

However, large differences in thermal and physical properties of indium and iron result in difficult manufacture of indium/iron composite. The traditional method to prepare the indium/iron composite plate is electroplate, which is relatively expensive and unable to manufacture the large composite plate. Therefore, explosive welding is proposed. Explosive welding is a solid-state welding technique, which is generally used to bond similar and dissimilar metal plates[5] through metallurgical bonding by high-speed oblique collision caused by the explosive energy. The usual explosive welding device has a flyer plate above the base plate with a certain distance, while the explosive is set on the top of the flyer plate with a detonator at one end of the edge. During the explosive welding process, the flyer plate accelerates to a very high velocity by the explosive products across the gap and obliquely collides with the base plate[6]. During this process, the metal jets are formed under high pressure and temperature, which can clean the plate surface[7]. Due to the collision and

Received date: June 10, 2022
Foundation item: National Science Foundation for Young Scientists of China (12102427, 12102202); Foundation of National Key Laboratory of Transient Physics (6142604210401)
Corresponding author: Wang Jinxiang, Ph. D., Professor, Nanjing University of Science and Technology, Nanjing 210094, P. R. China, Tel: 0086-25-84315276, E-mail: wjx@njust.edu.cn

the interaction among the jets, flyer plate and base plate, the obvious deformation occurs for the materials adjacent to the newly formed interface, and accordingly a wave-shape interface is formed between plates[8].

Compared with other welding methods, explosive welding has the advantage of high bonding strength and it can bond large plates in a single operation and maintain the initial physical and chemical properties of plates[9–10]. Thus, the explosive welding method has been widely used in industrial fields. Liang et al[11] prepared the Al-1060/Cu-T2 composites by explosive welding and studied the microstructure and the formation evolution mechanism. Tang et al[12] prepared the Cu/Fe/Cu composite with large thickness by two times of explosive welding. Parchuri et al[13] studied the Mo/Cu clads prepared by explosive welding and investigated the shock wave damage on Mo/Cu clads. Khaustov et al[14] developed a combined method of calculation and experiments to determine the heat flow on the flyer plate produced by detonation products. Yang et al[9] manufactured the 316L/CuCrZr hollow plate by multi-process of explosive welding, laser welding, and tungsten inert gas welding. It is reported that the prepared 316L/CuCrZr hollow plate has fine microstructure and good mechanical properties.

However, the investigation of indium/iron composite plate prepared by explosive welding is rarely reported. Due to the considerable discrepancy in mechanical properties between indium and iron, the common explosive thickness is too small to achieve successful detonation. In addition, due to the low melting point and the low strength of indium, it is important to protect the indium plate from the heat and stress wave produced by explosive. Thus, another iron plate, namely the velocity-control plate, was applied in the study. The velocity-control plate was placed above the flyer plate. The length and width of velocity-control plate were equal to those of the flyer plate, while the thickness of velocity-control plate was adjustable for the velocity control of flyer plate. Besides, the velocity-control plate can also protect the flyer plate from external heat and explosive energy.

To further investigate the modified explosive welding, experimental and numerical methods were both adopted to study the microstructure and mechanical properties of the indium/iron composite interface. The explosive welding parameters were calculated by the theoretic analysis. The interfacial microstructure was investigated by the optical microscope (OM). Meanwhile, the bending strength and shear strength of the interface were studied by standard mechanical properties tests.

1 Experiment and Numerical Simulation

1.1 Materials

In this research, three couples of commercially pure iron and indium plates were used, and their chemical composition is shown in Table 1 and Table 2, respectively. Due the mechanical and chemical properties of indium and iron, the indium and iron plates were set the flyer and base plates, respectively. The dimension of indium plate and iron plate was 200 mm×120 mm×3 mm and 200 mm×120 mm×10 mm, respectively. The ammonium nitrate/fuel oil explosive was adopted and its density is 0.8 g/cm^3. The detonation velocity was 2100 m/s.

1.2 Calculation of experiment parameters

The physical and mechanical properties of indium and iron plates are shown in Table 3. The schematic diagram of the explosive welding in this research is shown in Fig.1, where β is the collision angle, v_p is the collision velocity, and v_c is the collision point velocity. These three parameters are the main dynamic parameters for explosive welding. The relationship among β, v_p, and v_c can be expressed by Eq.(1)[15], as follows:

$$v_p = 2v_c \sin\left(\beta/2\right) \tag{1}$$

Only two parameters are independent. In this research, the collision velocity v_p and collision point velocity v_c were the dynamic conditions to determine the initial parameters of explosive welding. In order to form the jets between the plates during collision, the collision velocity v_c must be larger than the minimum collision velocity v_{pmin}, which can be calculated by Eq.(2–4)[16–17], as follows:

$$u_i = k\sqrt{\frac{H_i}{\rho_i}} \tag{2}$$

$$u_i = \frac{\sqrt{1+\frac{4\lambda_i P_{\min,i}}{\rho_i {C_{0,i}}^2}}-1}{\lambda_i} C_{0,i} \tag{3}$$

$$v_{pmin} = \frac{u_1 + u_2}{2} \tag{4}$$

Table 1 Chemical composition of iron plate (wt%)

C	S	P	Si	Mn	Al	Ni	Cu	Fe
0.01	0.01	0.01	0.02	0.02	0.01	0.01	0.01	99.90

Table 2 Chemical composition of indium plate (×10^{-4} wt%)

Cu	Al	Fe	Bi	Cd	Ti	Pb	Zn	Sn	As	Ni	In
1.1	0.5	2.0	3.0	0.5	3.0	2.8	1.3	3.0	3.0	0.5	Bal.

Table 3 Physical and mechanical properties of indium and iron

Material	Density, ρ/kg·m^{-3}	Tensile strength, σ_b/MPa	Hardness, HV/MPa	Sonic velocity, C_0/m·s^{-1}	Linear constant, λ	Specific heat, c/J·kg^{-1}·K^{-1}	Melting point, T_m/K
Indium	7300	4.5	10	2419	1.73	233	430
Iron	7900	166	150	4610	1.54	460	1805

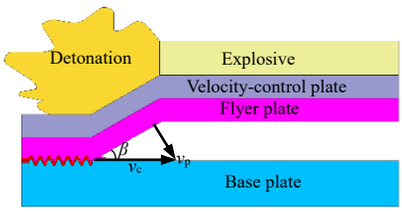

Fig.1 Schematic diagram of explosive welding

where k is a constant of 0.6 when the to-be-bonded surfaces are smooth; subscript i represents the flyer plate (i=1) or the base plate (i=2); λ is a linear constant of material; H_i, ρ_i, and $C_{0,i}$ are the Vickers hardness, density, and sonic velocity of flyer/base plate, respectively; $P_{\min,i}$ is the minimum weldable pressure of flyer/base plate; u_i is a related parameter of flyer/base plate. Based on Eq. (2) and Eq. (3), the minimum weldable pressure of flyer/base plate can be calculated. Then, the larger $P_{\min,i}$ is set as the minimum weldable pressure of the composite plate system $P_{\min}$. Sequentially, substitute $P_{\min}$ for $P_{\min,i}$ in Eq.(3) to obtain the final u_i of flyer/base plate. Finally, the minimum collision velocity of composite plate can be calculated based on the final u_1 and u_2.

Meanwhile, in order to ensure the formation of jets, the pressure of the collision point must be 10–12 times larger than the strength of composite plate, which is set as the strength of material with the higher strength between indium and iron, and the collision velocity at this moment is called as the flow limit V_{cmin}. Furthermore, the moving speed of the collision point must be lower than the sound speed of materials, namely the sound speed limit V_{cmax}. V_{cmin} and V_{cmax} can be determined by Eq.(5) and Eq.(6)[18], respectively:

$$V_{\text{cmax}} = C_{0,\min} \tag{5}$$

$$V_{\text{cmin}} = \sqrt{\frac{20\sigma_{\text{bmax}}}{\rho_{\min}}} \tag{6}$$

where $C_{0,\min}$ is the minimum sound velocity of the materials; $\rho_{\min}$ and σ_{bmax} are the smaller density and the larger static strength of indium and iron plates, respectively.

The higher limit of collision velocity for explosive welding is set as V_{pmax}. The over-melting phenomenon may occur in the interface when the collision velocity is higher than the maximum collision velocity. The maximum collision velocity of the flyer plate can be determined by Eq.(7)[19], as follows:

$$V_{\text{pmax}} = \frac{2\sqrt{2}-1}{\sqrt{N}\,v_{\text{D}}}\left[\left(T_{\text{m}}-T_0\right)^2\frac{\pi\gamma c C_0^{\,4}}{c_1\rho_1 h_1}\left(\frac{h_1+h_1}{h_2}\right)^2\right]^{\frac{1}{4}} \tag{7}$$

where N is a constant of 0.039; v_{D} is the detonation velocity of the explosive; T_{m}, γ, and c are the lowest melting point, thermal conductivity, and specific heat of materials, respectively; T_0 is the room temperature; C_0 and c_1 are sound velocity and volume wave velocity of the flyer plate, respectively; h_1 and h_2 are the thickness of the flyer plate and base plate, respectively.

In this research, the gap size δ can be determined by empirical formula, as follows:

$$\delta = 0.2\left(h_1 + h_2 + t_{\text{s}}\right) \tag{8}$$

where t_{s} is the thickness of the velocity-control plate.

The charge ratio R can be determined by Gurney formula[20], as follows:

$$v_{\text{p}} = \sqrt{2E}\left[\frac{3R}{5+R+4/R}\right]^{\frac{1}{2}} \tag{9}$$

where $\sqrt{2E}$ is Gurney energy. Gurney energy[21] can be determined by Eq.(10), as follows:

$$\sqrt{2E} = v_{\text{D}}\sqrt{\frac{2}{(\gamma^2-1)}\left(\frac{\gamma}{\gamma+1}\right)^{\gamma}} \tag{10}$$

where γ is the explosive polytropic exponent.

Because the velocity-control plate moves with the flyer plate, R can be determined by Eq.(11), as follows:

$$R = \rho_{\text{D}}h_{\text{D}}/\left(\rho_1 h_1 + \rho_{\text{s}}t_{\text{s}}\right) \tag{11}$$

where ρ_{D} and ρ_{s} are the density of the explosive and velocity-control plate, respectively; h_{D} is the explosive thickness. For the parallel explosive welding set, the collision point velocity v_{c} is equal to the detonation velocity v_{D}.

1.3 Numerical simulations

Numerical simulation was used to investigate the interfacial microstructure properties and the formation evolution mechanism[22–25], since the formation process is difficult to capture by experiment. In this research, the smoothed particle hydrodynamics (SPH) method was employed to reveal the explosive welding process with large strains. Through SPH method, the system state is represented by a set of particles with individual material properties, which obeys the governing conservation equations[26]. SPH particles are interpolation points, whose function values and derivatives can be estimated at the discrete points in the continuum[8].

The formulation of SPH can be divided into two key steps. The first step is the kernel approximation, namely the integration of the multiplication of an arbitrary function and a smoothing kernel function. The standard expression of the kernel approximation is as follows:

$$f(\boldsymbol{x}) = \int f(\boldsymbol{x}')W(\boldsymbol{x}-\boldsymbol{x}',h)\,\mathrm{d}\boldsymbol{x}' \tag{12}$$

where f is a function of the three-dimensional position vector $\boldsymbol{x}$; W is the kernel function depending on the distance $(\boldsymbol{x}-\boldsymbol{x}')$ and the smooth length h.

The second step is the particle approximation, which is the also the core step of SPH simulation, as follows:

$$f(\boldsymbol{x}_i) = \sum_{j=1}^{N}\frac{m_j}{\rho_j}f(\boldsymbol{x}_j)W(\boldsymbol{x}-\boldsymbol{x}',h) \tag{13}$$

where m_{j} and ρ_{j} are mass and density of the particle j, respectively; N is the total number of particles.

To verify the calculated parameters, a numerical explosive welding process was simulated by SPH method in AUTODYN software. The default units in AUTODYN software, such as the length unit (mm), the time unit (ms), and the mass unit (mg), were used. The explosive welding process was simplified to 2D oblique collision model to reduce simulation cost. Only indium and iron materials were employed, and the default parameters in the software were used. In the simulation model, the length of the indium and

iron plate was 5 mm, and the thickness of the indium plate was 3 mm, which was the same as the experiment value. The thickness of the iron plate was set as 0.7 mm to reduce computing cost. The initial conditions of the simulation were set in the form of the collision velocity and collision angle, as shown in Fig. 2. For the boundary set, the bottom of the iron plate with height of 0.4 mm was fixed along the thickness direction.

Since the particle size has a significant influence on the formation of bonding interface, the minimum and maximum sizes of SPH particles were set as 1 and 20 μm, respectively. The total number of SPH particles was 1 347 504. According to the explosive welding parameters, three initial conditions were selected and the corresponding resultant specimens were named as Clad 1, Clad 2, and Clad 3, as shown in Table 4.

1.4 Experiment

The schematic diagram of the experiment device is shown in Fig. 3. A velocity-control plate was put above the indium plate, and the industrial oil as the thermal barrier was filled in the gap of about 0.2 mm. Additionally, the application of the thermal barrier could prevent the bonding between the flyer plate and velocity-control plate. The gap size between the indium and iron plates in all conditions was set as 5 mm. The whole experiment set was placed on a steel anvil, as shown in Fig. 4. The explosive was triggered by the detonator to drive the flyer plate to collide with the base plate at the proper velocity.

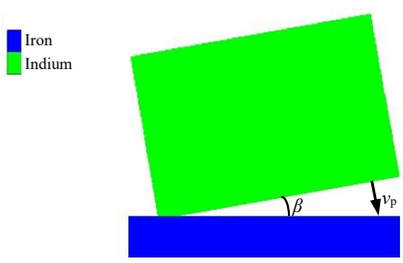

Fig.2 Schematic diagram of numerical calculation model

Table 4 Numerical simulation parameters under different initial conditions

Clad	Collision velocity, v_p/m·s^{-1}	Collision angle, β/(°)
1	190	8
2	210	10
3	240	13

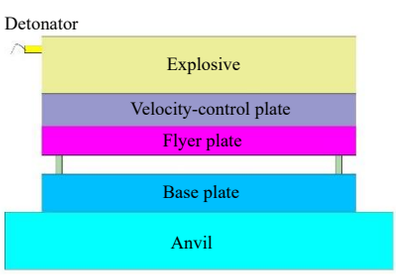

Fig.3 Schematic diagram of explosive welding experiment device

According to the physical and mechanical properties in Table 3, the designed explosive welding parameters were close to the lower limit of the dynamic parameters for the good quality of the obtained weldments. Three sets of parameters were determined, as shown in Table 5. With the protection of the velocity-control plate, the explosive welding process was conducted successfully. To observe the microstructure, the specimens were cut parallelly to the detonation direction. To investigate the mechanical properties, the bending and shear tests were conducted. The specimens for bending tests were 130 mm×26 mm×13 mm in size, and those for shear tests were 65 mm×25 mm×13 mm in size.

2 Results and Discussion

2.1 Microstructures of bonding interface

Fig. 5 shows OM microstructures of the interfaces parallel to detonation direction of clad specimens under different

Fig.4 Appearance of experiment device of explosive welding

Table 5 Explosive welding parameters under different initial conditions

Clad	Thickness of velocity-control plate, t_s/mm	Explosive thickness, h_D/mm
1	4	10
2	5	13
3	5	15

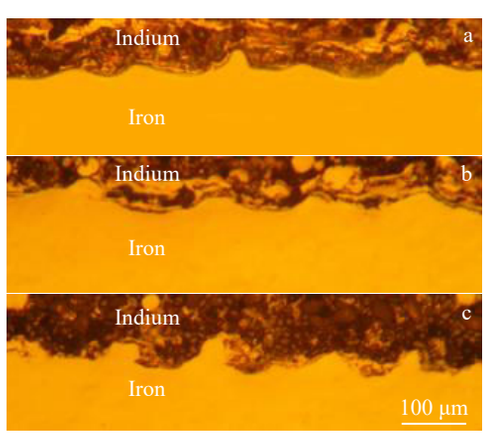

Fig.5 OM microstructures of interfaces parallel to detonation direction of Clad 1 (a), Clad 2 (b), and Clad 3 (c) specimens

initial conditions. All the clads present wave structures without defects, such as cracks or pores, which is consist with the results in Ref. [9,27]. The average wavelength in Clad 1, Clad 2, and Clad 3 is 101.6, 109.2, and 119.7 μm, while the average amplitude is 23.5, 27.5, and 35.2 μm, respectively. Different wave sizes can be attributed to the increasing thickness of explosive, i.e., the larger the explosive thickness, the larger the wavelength and amplitude[27]. Fig. 6 shows the microstructures of the single wave observed by optical microcope (OM), indicating that there are mixing regions adjacent to the bonding interface. This result is consistent with the results in Ref. [28]. During the collision, the direction of the jets is deflected and the jets crash into the surfaces of indium and iron plates. Afterwards, the jets slow down and are cut down by the deformed plates. Due to the low temperature and low strength of the indium material, the shape of the cut-down parts are irregular. Thus, no vortex-shape zone forms in the bonding interface, whereas the irregular areas can be obtained[11].

The wave structures are more beneficial to the mechanical properties and bonding area expansion than the straight ones. During the collision, the kinetic energy is deposited at the interface, which results in the rise of temperature and pressure. The metal jets form in front of the collision point to sweep the compounds out of the collision zone, providing a well-cleaned to-be-bonded surface, namely the self-cleaning phenomenon[29]. The huge plastic deformation occurs at the both sides of the indium and iron plates during the collision, forming the typical wave structures.

2.2 Microstructures of bonding interface

The explosive welding simulations under different initial conditions were conducted, and the jet generation can be observed, as shown in Fig. 7. Most jets are generated from the iron plate, which is consistent with the results in Ref. [24]. The jets crash into the surfaces and sweep away the metal particles. Moreover, the periodic oscillation of liquid metal jets is the premise for the formation of wavy interface[30]. In the numerical simulations, the wave sizes under different initial conditions are shown in Table 6. Meanwhile, the mixing regions with irregular shapes adjacent to the wavy interface are shown in Fig. 8, which are consistent with the experiment results. The experimental wave structures are similar to those of the simulation results.

The pressure of the explosive welding process was also studied. High pressure promotes the formation of jets during the collision. Fig. 9 shows the pressure contour of bonding plates. It can be seen that the pressure at the collision point is higher than that at other areas, and the maximum pressure is about 8 GPa, which is higher than the dynamic strength of materials. Thus, the composite plate exhibits the flow state for a short time, leading to the jet formation. Meanwhile, with the collision point moving, the pressure is decreased gradually.

Fig. 10 shows the contour of effective plastic strain of

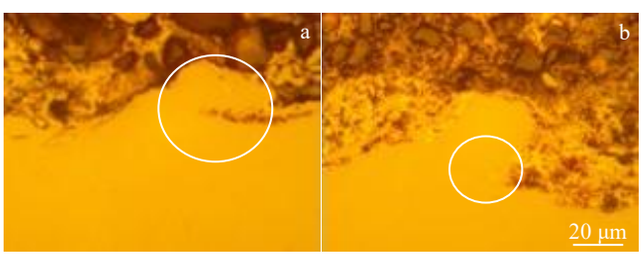

Fig.6 OM microstructures of single wave in mixing regions near the bonding interface

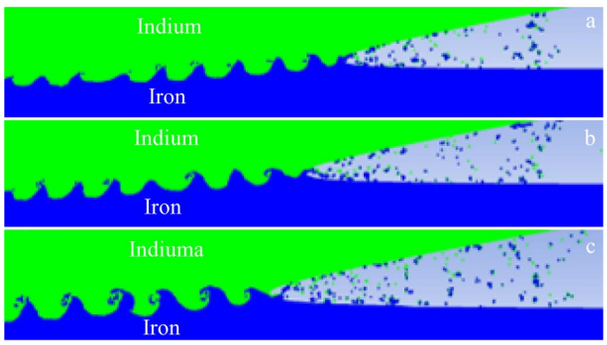

Fig.7 Simulated generation of jets and wave structures in Clad 1 (a), Clad 2 (b), and Clad 3 (c)

Table 6 Simulated parameters of interfacial microstructures under different initial conditions

Clad	Wavelength/μm	Amplitude/μm
1	101.1	25.1
2	107.5	31.7
3	118.2	37.3

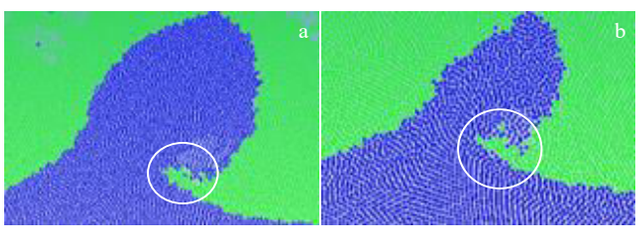

Fig.8 Simulated generation of irregular mixing areas

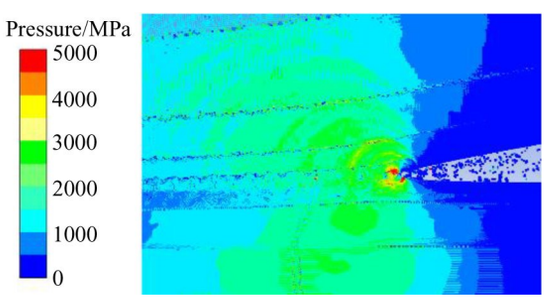

Fig.9 Simulated pressure distribution of bonding plate after explosive welding process

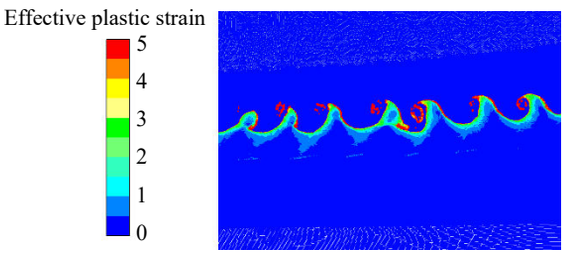

Fig.10 Simulated effective plastic strain distribution of bonding plate after explosive welding process

bonding plate. A narrow region of effective plastic strain can be observed adjacent to the bonding interface, which is consistent with the results in Ref. [31]. The large plastic deformation causes the large plastic strain near the interface. It can also be observed that a large effective plastic strain occurs in the mixing region, suggesting that a strong deformation occurs to form the mixing region.

2.3 Bending test

Three-point-bending tests were applied to examine the bonding strength of composite plate. The prepared plates were bent into an arc shape with the angle of about 90° under different conditions. The iron plate is at the inner corner side, as shown in Fig.11.

In the bending area, the plates are not separated and no crack or pore appears. However, due to the low strength, the indium plate under the external force is easily flattened. This result reveals that the indium/iron composite plate prepared by explosive welding can be easily deformed and shaped, showing great potential in manufacture of complex parts.

2.4 Shear test

To assess the bonding strength of the joining interface, the shear tests were conducted. The specimen appearances before and after the shear test are shown in Fig.12. The crack appears on one side of the bonding interface under the external force. With increasing the load, the crack spreads along the interface, causing the final separation. These phenomena reveal that the average shear strength of the composite plate is 16 MPa. Thus, the strength of bonding interface is stronger than that of the indium plate, which is consistent with the results in Ref.[32–33].

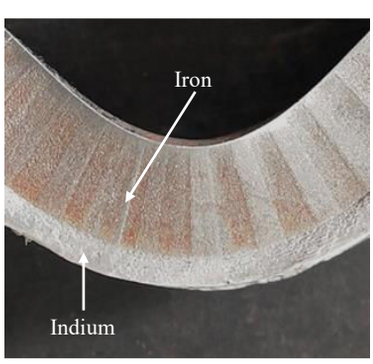

Fig.11 Appearance of bended indium/iron composite plate

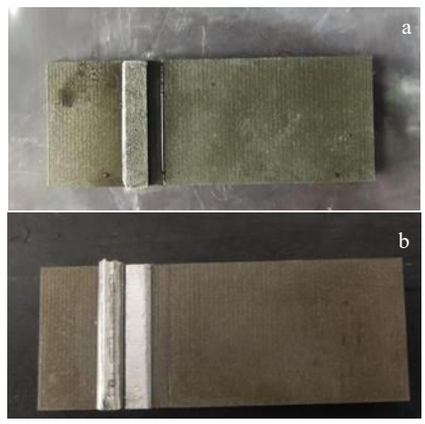

Fig.12 Appearances of indium/iron composite plate before (a) and after (b) shear test

3 Conclusions

1) The explosive welding by adding a velocity-control plate between the flyer plate and base plate is an effective method to prepare the indium/iron composite plate. High-quality wavy interfaces without defects can be formed under different explosive loads.

2) The microstructures of the indium/iron interface are related to the explosive loads. The wavelength and amplitude are increased with increasing the explosive thickness.

3) The simulation parameters calculated by theoretical analysis are verified. During the explosive welding process, the jets and mixing regions are formed. The maximum pressure exists in the area near the collision point. With the collision point moving, the pressure is decreased. In addition, a narrow large strain region exists in the collision zone.

4) The indium/iron interface has good mechanical properties. The composite plates after bending to 90° show no separation or crack. The shear strength of the indium/iron bonding interface is 16 MPa.

References

1 Pradhan D, Panda S, Sukla L B. *Mineral Processing and Extractive Metallurgy Review*[J], 2018, 39(3): 167
2 Ma X, Li L F, Zhang Z H *et al*. *Rare Metals*[J], 2015, 34(5): 324
3 Yin B, Lou C G. *Rare Metals*[J], 2015, 34(7): 510
4 Gunn G. *Critical Metals Handbook*[M]. Hoboken: John Wiley & Sons, 2014: 204
5 Akbari-Mousavi S, Barrett L M, Al-Hassani S. *Journal of Materials Processing Technology*[J], 2008, 202(1–3): 224
6 Song J, Kostka A, Veehmayer M *et al*. *Materials Science and Engineering A*[J], 2011, 528(6): 2641
7 Findik F. *Materials & Design*[J], 2011, 32(3): 1081
8 Chu Q L, Min Z, Li J H *et al*. *Materials Science and Engineering A*[J], 2017, 689: 323
9 Yang M, Ma H H, Yao D M *et al*. *Fusion Engineering and Design*[J], 2019, 144: 107

10 Yang M, Ma H H, Shen Z W. *Journal of Materials Research and Technology*[J], 2019, 8(6): 5572
11 Liang H L, Luo N, Chen Y L *et al*. *Composite Interfaces*[J], 2021, 29(5): 465
12 Tang K, Wang J Z, Fang Y *et al*. *Rare Metal Materials and Engineering*[J], 2020, 49(5): 1553
13 Parchuri P, Kotegawa S, Ito K *et al*. *Metals*[J], 2021, 11(3): 501
14 Khaustov S V, Pai V V, Lukyanov Y L *et al*. *International Journal of Heat and Mass Transfer*[J], 2020, 163: 120 469
15 Saravanan S, Raghukandan K. *Advanced Materials Research*[J], 2012, 445: 729
16 Wang X, Gu C X, Zheng Y Y *et al*. *Materials & Design*[J], 2014, 56: 26
17 Crossland B, Williams J D. *Metallurgical Reviews*[J], 1970, 15(1): 79
18 Ribeiro J B, Mendes R, Loureiro A. *Journal of Physics Conference*[J], 2014, 500(5): 52 038
19 Deng Wei, Lu Ming, Tian Xiaojie. *Explosion and Shock Waves* [J], 2015, 35(1): 82 (in Chinese)
20 Gulenc B. *Materials & Design*[J], 2008, 29(1): 275
21 Koch A, Arnold N, Estermann M. *Propellants, Explosives, Pyrotechnics*[J], 2002, 27(6): 365
22 Li Y, Liu C R, Yu H B *et al*. *Metals*[J], 2017, 7(10): 407
23 Sun Z R, Shi C G, Xu F *et al*. *Materials & Design*[J], 2020, 191: 108 630
24 Mousavi S A A A, Al-Hassani S T S. *Materials & Design*[J], 2008, 29(1): 1
25 Liang H, Luo N, Tao S *et al*. *Journal of Materials Research and Technology*[J], 2020, 9(2): 1539
26 Liu G R, Liu M B. *Smoothed Particle Hydrodynamics: A Meshfree Particle Method*[M]. Singapore: World Scientific, 2003: 26
27 Yang M, Ma H H, Shen Z W. *Propellants, Explosives, Pyrotechnics*[J], 2019, 44(5): 609
28 Zhao H, Sheng L Y. *Journal of Manufacturing Processes*[J], 2021, 64: 265
29 Bataev I A, Tanaka S, Zhou Q *et al*. *Materials & Design*[J], 2019, 169: 107 649
30 Han Shunchang. *Phase Transformation and Fractography of Interface of Explosive Welding*[M]. Beijing: National Defense Industry Press, 2011: 2 (in Chinese)
31 Nassiri A, Kinsey B. *Journal of Manufacturing Processes*[J], 2016, 24(2): 376
32 Asemabadi M, Sedighi M, Honarpisheh M. *Materials Science and Engineering A*[J], 2012, 558: 144
33 Athar M M H, Tolaminejad B. *Materials & Design*[J], 2015, 86: 516

爆炸焊接法制备铌/铁复合板的实验与数值模拟

曹　超[1]，王金相[1]，杨　明[1]，唐　奎[1]，方　雨[2]
(1. 南京理工大学 瞬态物理国家重点实验室，江苏 南京 210094)
(2. 安徽弘雷金属复合材料科技有限公司，安徽 宣城 242000)

摘　要：提出了一种通过在炸药与复合板之间增加一层速度调整板，以获得理想焊接条件的用于制备铌/铁复合板的新型爆炸焊接方法。通过理论方法计算了爆炸焊接参数，通过实验对炸药载荷的影响进行了研究。应用光滑粒子流体动力学（SPH）方法进行数值模拟以验证参数有效性，探究了结合界面的成型机理，并研究了压力和塑性应变的分布。结果表明，当炸药厚度增加时，界面波形结构更明显。界面剪切试验结果表明铌/铁复合板结合面抗剪切强度为16 MPa，比纯铌材料的抗剪切强度高，且三点弯曲试验之后复合板结合界面无裂纹。采用改进的爆炸焊接方法可以有效制备高质量铌/铁复合板。

关键词：爆炸焊接；铌/铁复合板；速度调整板；SPH模拟

作者简介：曹　超，男，1999年生，博士生，南京理工大学瞬态物理国家重点实验室，江苏 南京 210094，电话：025-84315276，E-mail：918101630106@njust.edu.cn